

Effect of pulse laser treatment at different process variables on mechanical behavior of carbon nanotubes electrophoretically deposited on titanium alloy

BEATA MAJKOWSKA-MARZEC*, KACPER STASZEWSKI, JOANNA SYPNIEWSKA

Gdańsk University of Technology, Faculty of Mechanical Engineering and Ship Technology,
Department of Biomaterials Technology, Gdańsk, Poland.

Purpose: Titanium and its alloys are widely used as biomaterials for long-term implants, but they are usually surface-modified due to their weak bioactivity and wear resistance. Laser processing was used to modify the surface layer, and elemental carbon was a component of the deposited coatings. This research aims to use a combination of both methods based on preliminary electrophoretic deposition of multi-wall carbon nanotubes (MWCNTs) followed by pulse laser treatment. Carbon nanotubes were chosen due to their mechanical and chemical stability as well as their tubular shape, resulting in enhanced mechanical properties of laser-modified layers. *Methods:* The pulse laser power and laser scanning speed were defined as variable process parameters. The microstructure, roughness R_a , nanohardness H , Young's modulus E , and indent depth values were measured, and the H/E , H^3/E^2 , and relative changes of all these values in comparison to MWCNTs-coated and non-coated surfaces, were calculated. *Results:* The obtained results show that the best mechanical properties of MWCNTs-coated and laser-treated specimens are obtained at a laser power of 900 W and laser feed of 6 mm/s. The observed relations can be explained considering processes occurring on the surface such as deposition of carbon nanotubes, melting and re-crystallization of the surface layer, formation and possible partial decomposition of titanium carbides, and associated changes in local chemical composition, phase composition, and a level of residual stresses beneath the surface. *Conclusions:* The developed process can substitute the time and money-consuming carbonization of titanium and its alloys.

Key words: Ti13Nb13Zr alloy, laser modification, multiwall carbon nanotubes, roughness, nanohardness, Young's modulus

1. Introduction

The commonly used Ti-based materials include titanium of technical purity, Ti6Al4V, Ti6Al7Nb, and seldom Ti13Nb13Zr alloy, the last now especially promising for medicine because of its safe chemical composition, high biocompatibility, Young's modulus approaching a value for a cortical bone, and moderate mechanical properties.

Titanium and its alloys are often subjected to surface modification to improve their hardness, fatigue and corrosion fatigue limits, wear and fretting resistance, corrosion resistance in aggressive solutions, and to enhance several biological properties such as bioac-

tivity and antibacterial efficiency. The usually applied techniques include mechanical hardening, chemical treatment, oxidation, ion plasma implantation, electrophoretic deposition, spark plasma sintering, plasma spraying of coatings and rapidly developed laser treatment [16], [23], [27]. Among different coatings deposited on titanium surfaces and on other metallic materials, the carbon nanotubes were several times deposited on titanium [12], [24], Ti6Al4V [8], [15] and Ti13Nb13Zr alloy [26].

The laser treatment of metals is a very common surface modification technique [1], [18] used to change the surface topography, the microstructure within the remelted zone, and the phase and chemical composition of the subsurface zone. They can affect hydrophilicity,

* Corresponding author: Beata Majkowska-Marzec, Gdańsk University of Technology, Faculty of Mechanical Engineering and Ship Technology, Department of Biomaterials Technology, ul. Narutowicza 11/12, 80-233 Gdańsk, Poland. E-mail: beata.majkowska@pg.edu.pl

Received: August 8th, 2023

Accepted for publication: October 13th, 2023

bioactivity, and adhesion of other layers. The laser treatment was already used for titanium and its alloys for different purposes. Selective laser melting was often applied to obtain the titanium scaffolds [37]. Laser cladding is likely the most popular among laser modifications of titanium alloys, used for the fabrication of the composite coating of TiC and Ni alloy [5], [35], and Ti-Al-Nb-2Mn alloys on TiAl intermetallic [32]. The laser shock peening is quite often useful for modification of Ti6Al4V alloy, with or without a protective layer [25], [39], or for Ti6Al4V samples with micro-dimple arrays in contact with foil [9].

The CNTs were subjected to some laser-enhanced processes. They were included in several composites as the 316L stainless steel manufactured together with CNTs by laser-assisted additive manufacturing [36], composite powders with CNTs applied for laser printing of electronics [29], the CNTs-SiC reinforced aluminum fabricated by laser melting injection [33] and composite coatings of polymers and SWCNTs for cardiovascular implants [11]. Nanocomposites of MWCNTs decorated with ZnO nanoparticles were prepared by Nd:YAG laser [2], MWCNTs decorated with SnO₂ nanoparticles for photocatalytic applications by pulsed laser ablation [4]. For coatings, the Ti₃O₅ nanofilm was formed on CNTs by pulse laser deposition for improvement of the electrochemical behavior [30], oxide layers containing carbon nanotubes on Al alloy [31], and laser beam lithography of carbon nanotube arrays became useful in the manufacturing of field electron emitters [13]. The laser-induced surface patterns were obtained based on the transfer of thermal energy at the interface between the carbon nanotubes and the polymer [8].

Even if the carbon nanotubes have been used for different purposes in the processes of surface laser treatment or welding or fabrication of composite materials, the idea of a two-stage process, i.e., (i) deposition of CNT-coating subsequently followed by (ii) its remelting and solidification, has never been presented except for several our previous investigations [21], [22]. The concept is that the laser treatment can cause the melting of the surface layer, and diffusion of carbon atoms at elevated temperatures, in liquid, and adjacent solid areas, resulting, among others, in the appearance of titanium carbides. Such a process should result in the improvement of surface mechanical properties significantly dependent on laser energy density which

determines the solid-to-liquid transformation kinetics, diffusion kinetics, and carbides' precipitation kinetics. In effect, this process is similar to the carbonization of titanium materials. The advantage of our novel technique over carbonization is in a much shorter time and has fewer expenses. Besides, the possibility to design and obtain the surface-modified titanium exactly for the demanded purpose, according to several adjusted parameters such as overall laser power, pulse power, time, frequency, and scanning overpassing percentage, is another advantage. The present research proposes an improvement of surface properties, in particular hardness and Young's modulus, comprising the electrophoretic deposition of multi-wall carbon nanotubes (MWCNTs) on the Ti13Zr13Nb alloy, followed by pulse laser treatment at moderate laser surface restructuring. The research hypothesis sounds that the optimal values of pulse laser power and laser scan rate can change the microstructure of the surface layer determined by the specific laser influence resulting in the highly plausible mechanical characteristics of the surface.

2. Materials and methods

The chemical composition of the base material, Ti13Nb13Zr alloy, based on a certificate of the delivering company (Xi'an SAITE Metal Materials Development Co., Ltd., Xi'an, China) is given in Table 1.

To acquire suitable roughness and remove surface imperfections, the samples were polished using SiC sandpapers of grades 220, 500, and 800 (Struers Comp., Poland). Grinding was carried out by wet method with a metallographic grinder-polisher (Saphir 330, ATM GmbH, Germany). Then the specimens were washed in tap water, dried in an air stream, washed with acetone for 120 s, rinsed with distilled water, etched in 5% hydrofluoric acid for 30 s, and again rinsed with distilled water.

To prepare the coating, multiwall carbon nanotubes (3D-Nano, Krakow, Poland) were functionalized according to [20], resulting in achieving the suspension of 0.31 wt. % CNTs in water. Then, the obtained suspension was diluted with 40 mL of distilled water to get a concentration of CNTs of about 0.16 wt. %, which gave the best results based on our latest tests.

Table 1. Chemical composition of the Ti13Nb13Zr alloy, wt. %

Element	C	Fe	Nb	Zr	O	S	H	N	Ti
Content, wt. %	0.035	0.085	13.18	13.49	0.078	<0.001	0.055	0.019	73.06

Obtained suspensions were subjected to ultrasonic homogenization for 30 min to separate the CNTs, before the electrophoretic deposition process. Functionalization of CNTs makes the process of their deposition by EPD faster and easier.

The electrophoretic deposition (EPD) technique was applied to obtain the coatings under a voltage of 20 V (DC power source by the MCP/SPN110-01C, Shanghai MCP Corp., Shanghai, China) and deposition time of 30 s, at ambient temperature. As the anode, the Ti13Nb13Zr substrate was used, and stainless steel served as a counter electrode. The electrodes were put into liquid, parallel to each other, 10 mm apart. The freshly produced coatings remained in the ambient air for 24 h before the tests started.

Prepared samples were laser modified using the Nd:YAG pulse laser (TruLaser Station 5004, TRUMPF, Germany) emits a beam with a wavelength of 1064 nm under a shielding argon gas with the parameters shown in Table 2. In the applied designation of the sample (Table 2), TNZ means the Ti13Nb13Zr alloy only polished, CNT means the sample polished and deposited with CNTs, L the sample polished and laser-treated, CL the sample polished, deposited with CNTs and laser processed. The numeric symbols mean: number before a dash means the laser pulse power expressed in hundreds of watts, and that after the dash is the laser scanning speed in mm/s.

Table 2. Designations of the samples and corresponding process parameters of their laser processing

Sample's designation	Presence of CNTs coating	Power of the laser pulse [W]	Laser scanning speed [mm/s]
TNZ	–	–	–
CNT	+		
L7-3	–	700	3
CL7-3	+		
L7-6	–		6
CL7-6	+		
*L8-3	–	800	3
*CL8-3	+		
*L8-6	–		6
*CL8-6	+		
L9-3	–	900	3
CL9-3	+		
*L9-6	–		6
*CL9-6	+		
L20-3	–	2000	3
CL20-3	+		
L20-6	–		6
CL20-6	+		

The applied experimental plan was designed to estimate the effects of the following input variables:

the presence or absence of the CNTs layer, the laser power, and the laser scan rate (scanning speed). The output variables included roughness, indent depth, (nano)hardness, Young's modulus, and two calculated mechanical indices, H/E , and H^3/E^2 .

The surface and cross-sections of the modified samples were examined using both an optical microscope (Olympus UC 50, Hamburg, Germany) and a scanning electron microscope (SEM) (JEOL JSM-7800 F, Tokyo, Japan). The thickness of the laser-treated surface layer was determined from the analysis of cross-section images.

To identify the phases appearing in the modified samples, X-ray diffraction (XRD) analysis was employed with a Phillips X'Pert Pro instrument (Almelo, the Netherlands). This method utilized a diffractometer with Cu-K α radiation ($\lambda = 0.1554$ nm) within the 10–90 range of 2θ . The roughness R_a measurement was performed at a distance of 4 mm using a profilograph Hommel Etamic Waveline (JENOPTIK, Germany). Each value of the roughness R_a is an arithmetic mean from three measurements with standard deviation (SD) calculated.

Nanoindentation tests were performed using the NanoTest™ Vantage (Micro Materials, Great Britain) equipped with a Berkovich pyramidal diamond. For each specimen, twenty-five (5×5) measurements were made at the highest applied force of 50 mN, the loading and unloading times of 20 s, and the dwell period at the highest load of 10 s. The distances between the subsequent indents equaled to 20 μ m. Based on the Oliver and Pharr approach, the indent depth, the hardness (H), and the reduced Young's modulus (E_r) were determined. When estimating real elastic modulus (E), the Poisson's ratio values of 0.25 for CNTs coating and 0.36 for Ti alloy were implied.

3. Results

Several surface images of (i) a native material, (ii) CNTs coated, and several (iii) laser-treated, and (iv) CNTs-coated and laser-treated surface views are shown in Fig. 1.

Some examples of microstructures examined on the cross-sections for (i) several laser-treated, and (ii) CNTs-coated and laser-treated surface views, obtained by light microscope and SEM. As demonstrated by views of the cross-sections in Figure 2, the thickness of each laser-melted layer is indicated by a dashed line, and its value is provided in Table 3.

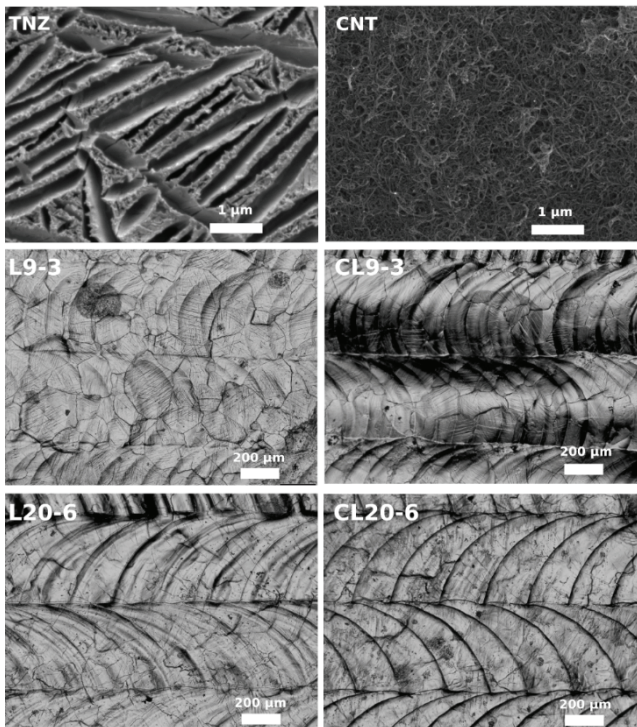


Fig. 1. Surface images of Ti13Nb13Zr alloy before laser treatment (TNZ), with CNTs coating (CNT), and several laser-treated (L9-3, L20-6), and CNTs-coated and laser treated (CL9-3, CL20-6). Scanning electron microscope SEM (TNZ and CNT) and light microscope LM (rest of the sample)

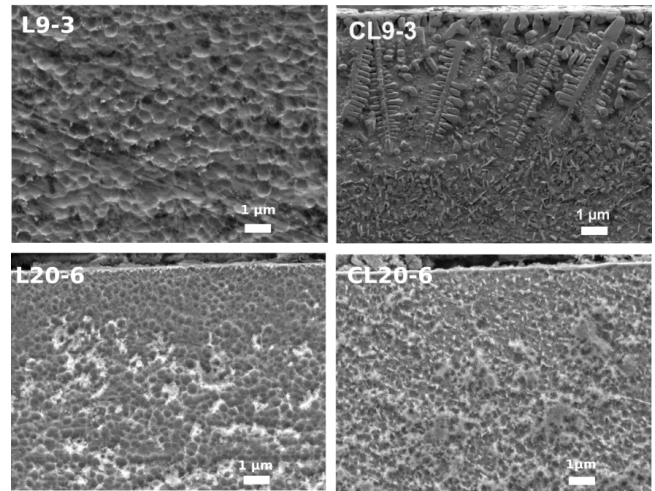


Fig. 3. Microstructures on cross-sections for several laser-treated, and CNTs-coated and laser-treated surface views of Ti13Nb13Zr alloy. Scanning electron microscope SEM

Table 3. The mean thickness and the corresponding standard deviation of laser-modified layers

Sample	Thickness ± SD [μm]
L9-3	88 ± 9
CL9-3	107 ± 25
L20-6	318 ± 36
CL20-6	384 ± 28

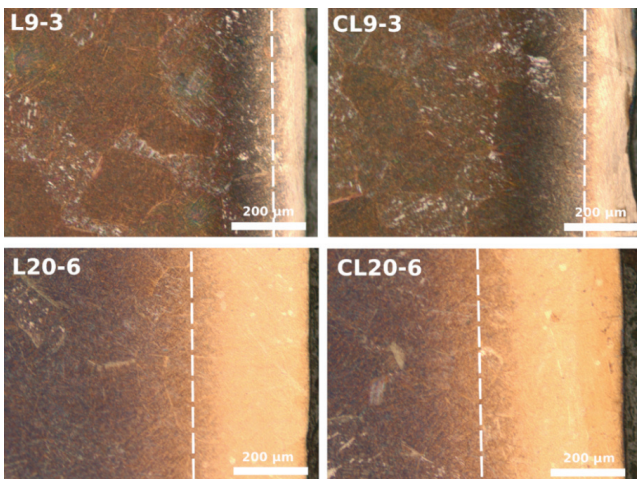


Fig. 2. Microstructures on cross-sections for several laser-treated, and CNTs-coated and laser-treated surface views of Ti13Nb13Zr alloy. Light microscope LM

XRD spectra for ground native material, which is Ti13Nb13Zr alloy (TNZ), L9-3 and L20-6 – for laser-treated material, CL9-3, and CL20-6 – for laser-treated material with a previously applied coating of carbon nanotubes, are presented in Fig. 4.

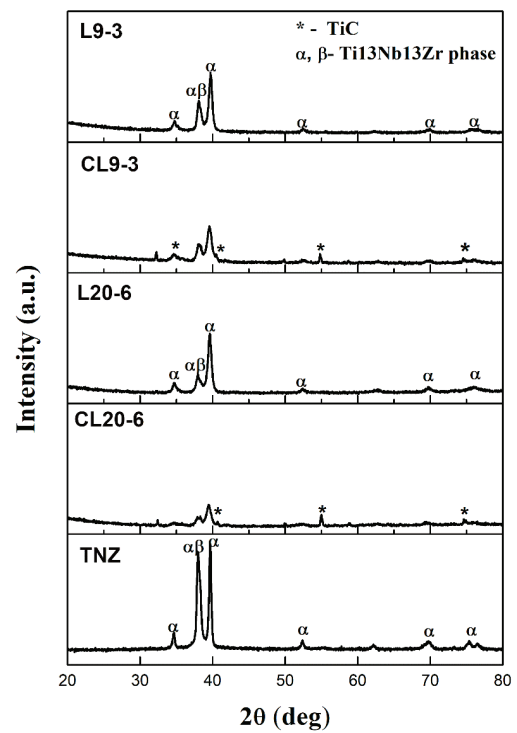


Fig. 4. XRD spectra of Ti13Nb13Zr alloy for: TNZ, L9-3 and L20-6 – samples after laser treatment, CL9-3 and CL20-6 – samples with CNTs coating after laser treatment

Table 4. The roughness of investigated samples for different process parameters

Designation of samples	Presence of CNTs coating	Power of the laser pulse [W]	Laser feed rate [mm/s]	Roughness [μm]
TNZ	–	–	–	0.23 ± 0.02
L7-3	–	700	3	1.67 ± 0.01
CL7-3	+			2.04 ± 0.03
L7-6	–		6	1.92 ± 0.02
CL7-6	+			1.97 ± 0.01
L9-3	–	900	3	0.87 ± 0.02
CL9-3	+			4.41 ± 0.04
L20-3	–	2000	3	1.73 ± 0.02
CL20-3	+			0.79 ± 0.01
L20-6	–		6	1.67 ± 0.02
CL20-6	+			1.40 ± 0.01

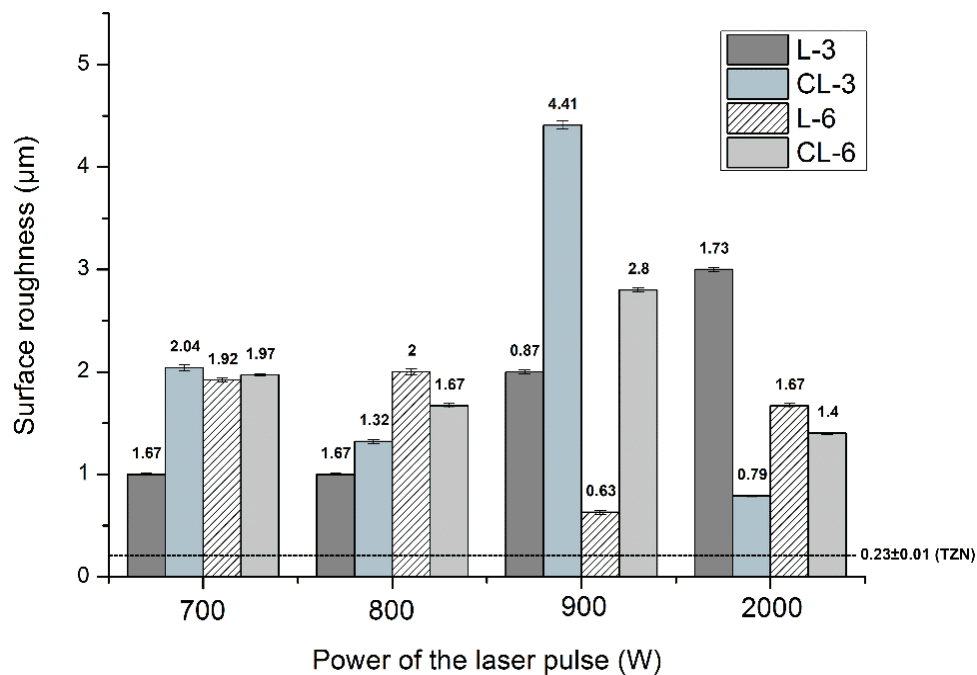


Fig. 5. Surface roughness of Ti13Nb13Zr alloy after laser treatment in different parameters with and without CNTs coatings

Table 5. Mechanical parameters of samples for different process parameters

Designation of samples	Presence of CNTs coating	Laser pulse power [W]	Laser feed rate [mm/s]	Nanohardness (H) [GPa]	Young's modulus (E) [GPa]
TNZ	–	–	–	20.62 ± 14.20	279.09 ± 134.39
CNT	+			0.35 ± 0.18	26.56 ± 8.03
L7-3	–	700	3	41.61 ± 11.83	370.71 ± 85.38
CL7-3	+			52.73 ± 10.98	395.01 ± 69.82
L7-6	–		6	46.82 ± 13.57	398.7 ± 99.22
CL7-6	+			34.25 ± 14.98	334.65 ± 123.43
L9-3	–	900	3	43.18 ± 19.92	350.91 ± 101.52
CL9-3	+			56.18 ± 21.08	405.35 ± 119.44
L20-3	–	2000	3	52.13 ± 12.13	342.54 ± 94.12
CL20-3	+			56.4 ± 11.42	359.18 ± 51.47
L20-6	–		6	65.48 ± 15.04	383.43 ± 84.12
CL20-6	+			55.19 ± 18.17	387.1 ± 111.89

The results of the present roughness measurements are demonstrated in Table 4. Similar results together with previous R_a values [21] obtained at 800 W, at 3 and 6 mm/s, and 900 W, at 6 mm/s, for laser power and scanning speed, respectively, are shown in Fig. 5.

obtained at 800 W at 3 and 6 mm/s, and at 900 W, at 6 mm/s, for laser power and scanning speed, respectively, are shown in Figs. 6 and 7.

In Table 6, the present results of measured indent depth, and values of two ratios, mainly H/E and H^3/E^2 ,

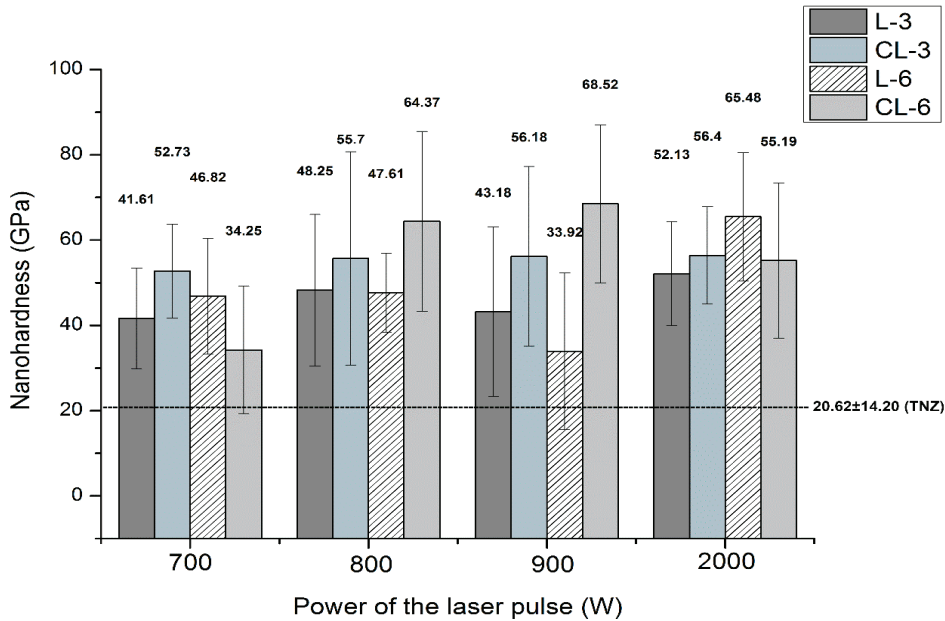


Fig. 6. Nanoindentation hardness of Ti13Nb13Zr alloy after laser treatment in different parameters with and without CNTs coatings (relationships between pulse laser power, scanning speed and hardness)

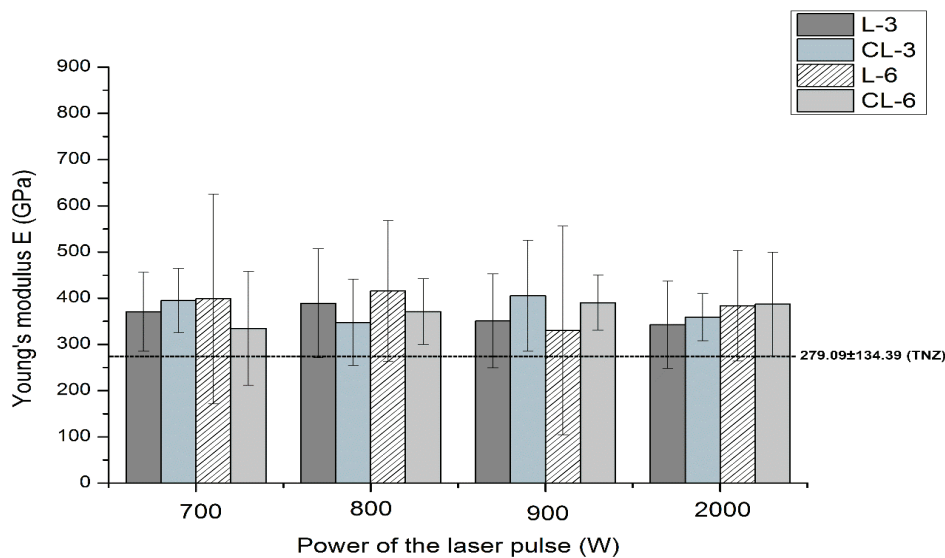


Fig. 7. Young's modulus values of Ti13Nb13Zr alloy laser-treated at different parameters, in a presence or absence of CNTs coating (relationships between pulse laser power, scanning speed and Young's modulus)

The present results of nanoindentation and Young's modulus measurements are demonstrated in Table 5. Similar results together with several earlier ones [21]

important for an assessment of resistance to elastic and plastic deformations based on (nano)hardness and Young's modulus values, are demonstrated.

The calculated values of both ratios, also for 800 W at 3 and 6 mm/s and 900 W, at 6 mm/s are presented, for laser power and scanning speed, respectively, which have been obtained in earlier work [21] are show in Figs. 8 and 9.

The fundamental aim of this research is to establish whether the deposition of CNTs coating can influence the mechanical behavior within the surface layer. The relative changes in measured parameters, CNTs-deposited and laser-processed (no index) com-

pared to those only laser-treated (index LT) are demonstrated in Table 7. It can be seen that the carbon nanotubes certainly increase the roughness at 900 W of laser power, increase the hardness at the same energy, and have a small or negligible (taking into account the high SDs values) effect on Young's modulus, for which only at 900 W the more significant effect can be observed. However, the increase in both plastic and elastic work is the highest at 900 W and the highest scanning speed.

Table 6. Maximum indent depth and fracture toughness measures, H/E and H^3/E^2

Designation of samples	Presence of CNTs coating	Power of the laser pulse [W]	Laser feed rate [mm/s]	Maximum indent depth [nm]	H/E [-]	H^3/E^2 [GPa]
TNZ	-	-	-	441.38 ± 197.49	0.074	0.113
CNT	+			2818.1 ± 402.03	0.013	0.00006
L7-3	-	700	3	268.98 ± 46.79	0.112	0.523
CL7-3	+			242.56 ± 26.41	0.133	0.936
L7-6	-		6	253.17 ± 38.32	0.117	0.641
CL7-6	+			340.06 ± 159.62	0.103	0.359
L9-3	-	900	3	290.31 ± 93.15	0.123	0.654
CL9-3	+			245.08 ± 47.94	0.139	1.082
L20-3	-	2000	3	268.21 ± 79.35	0.152	1.207
CL20-3	+			245.93 ± 24.87	0.157	1.39
L20-6	-		6	249.54 ± 80.29	0.171	1.909
CL20-6	+			247.55 ± 44.27	0.143	1.176

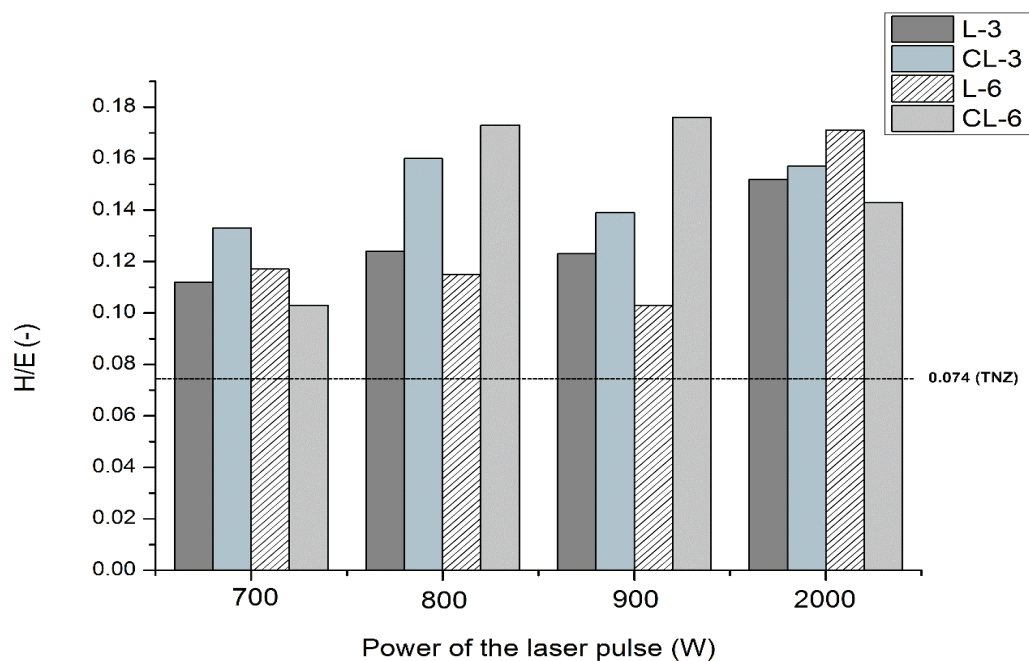


Fig. 8. The effect of pulse laser power on the H/E ratio for two applied laser feed values, with or without CNTs coating

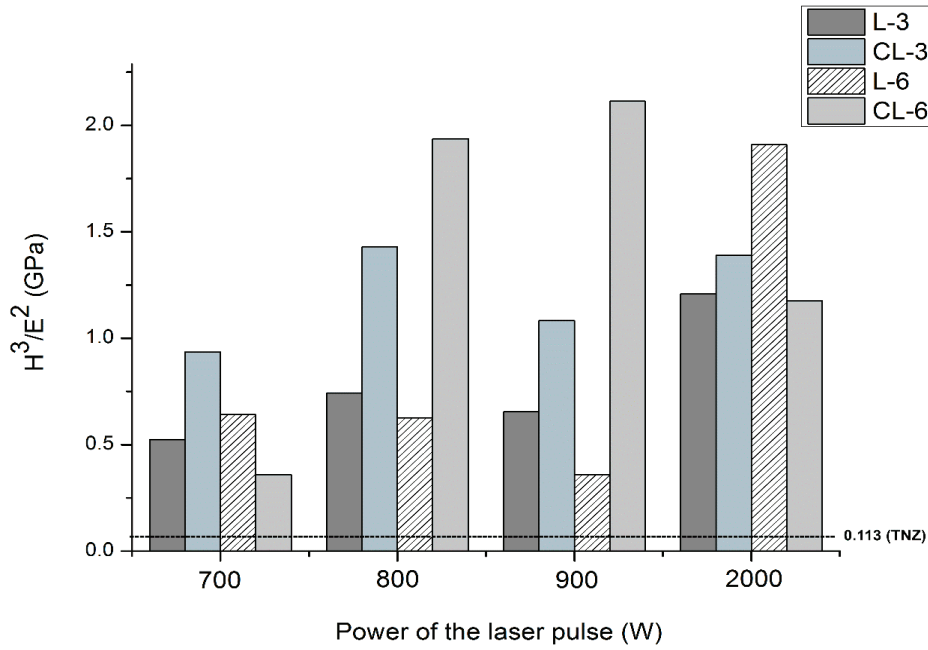


Fig. 9. The effect of pulse laser power on the H^3/E^2 ratio for two applied laser feed values, with or without CNTs coating

Table 7. Relative changes of measured parameters

Laser power [W]	Laser beam feed [mm/s]	$(R_a - R_{aLT})/R_{aLT}$ [%]	$(H - H_{LT})/H_{LT}$ [%]	$(E - E_{LT})/E_{LT}$ [%]	$(H/E) - (H_{LT}/E_{LT})/(H_{LT}/E_{LT})$ [%]	$(H^3/E^2) - (H_{LT}^3/E_{LT}^2)/(H_{LT}^3/E_{LT}^2)$ [%]
7000	3	22.2	26.7	6.6	18.7	79.0
	6	2.6	-26.8	-16.1	-11.9	-44.0
8000	3*	-19.2	15.4	-10.7	29	92.7
	6*	-16.5	35.2	-10.7	50.4	210
9000	3	407	30.1	15.5	13.0	65.4
	6*	344	102	18.2	70.8	492
20000	3	-54,3	8.2	4.8	3.2	15.1
	6	-16.2	-15.7	0.9	-16.4	-38.4

* values calculated based on previous results [21].

4. Discussion

In Figure 1, we can observe the path of laser tracks (for laser-modified samples), which corresponds to the direction of the laser head's movement. Surface melting and rapid solidification result in what is referred to as laser structuring, associated with a change in surface roughness. No cracks are observed in the resulting surface layers (Figs. 1 and 2). The adhesion of the carbon coating to the titanium substrate has been previously examined [20], confirming its suitability for use in titanium implants. Large surface irregularities and a zonal character of the laser-modified layer are also visible (Fig. 3).

The samples were tested by X-ray diffraction (XRD) (Fig. 4) analysis to demonstrate the presence of titanium carbides in the near-surface zone after electrophoretic deposition of the carbon coating, also visible in the form of dendrites in Fig. 3 (CL9-3).

As can be seen in Table 4 and Fig. 5, for only laser-processed samples, roughness is always much higher than for bare metal and is not significantly influenced by laser power, except 900 W at which roughness becomes twice lower than for the others, for 6 mm/s of scanning speed. For CNTs-coated and laser-treated alloy, the relation is more complex with minimum and maximum roughness observed at middle pulse laser power. Such observations can be satisfactorily explained. Namely, at low laser power, or high

scan rate, the sub-wavelength laser-induced periodic surface structures can appear [10]. On the contrary, at high laser power or low laser scanning speed, micro-cracks can initiate. The reported surface roughness has ranged between 143 nm and 326 nm, well below here observed values. However, under the effect of laser treatment, well-defined pits with hierarchic organization can be found on the surface, and these micro and nanoscale imperfections are induced by two processes, the re-solidification of the liquid metal, and the re-deposition of plasma plume [14]. The obtained results prove that in these tests such non-equilibrium processes are either very intensive, or temperature gradients are high, or quenching is particularly fast, or all these effects appear simultaneously.

It can be observed that surface hardness is higher for each surface-modified sample compared to that of bare metal (Table 5 and Fig. 6). The high standard deviations, even for only laser-treated samples, can be attributed to presumably high nonuniformity of the surface layer, following the surface melting process, diffusion of alloying elements in liquid melt, and rapid solidification resulted in the important stochastic movement of atoms under concentration, temperature and stress gradients, and gravitation force. For CNTs coated and laser-treated alloy, a significant increase in surface hardness was already observed and attributed to the microstructural change within the layer influenced by laser energy, such as the appearance of a layer of β -phase beneath the surface, the laser beam interaction with the titanium in plasma conditions, and the appearance of flower-like microstructural feature [6]. For the carbon-coated titanium irradiated with the Nd:YAG laser, the carbide coating was primarily affected by the scanning speed, and the hardness of the laser-modified samples occurred even 6 times higher than that of titanium [3]. In our research, such improvement is also observed, but the increase is distinctly lower, presumably because of CNTs used as a coating. Also, Young's modulus increases after any surface processing compared to the substrate. For CNTs-coated and laser-treated alloy, its value is the highest for pulse laser power of 900 W and 2000 W, again at higher scanning speed. The surface layer is then significantly hardened and strengthened at applied conditions.

Based on data collected in Table 6, it can be seen that the maximum indent depth is exceptionally high only for the CNTs coating alone, which might be expected for such a loose cover. The laser treatment, following the CNTs deposition or not, results in a significant decrease in the indent depth. All these values are well below the determined remelted zone depth. The

pulse laser power does not influence the indent depth for only laser-treated samples and any of the two scanning speed values. A similar effect is observed for two-stage processed samples, for which the hardness increases already at 900 W. However, the standard deviations are high and such a conclusion is disputable.

The H/E and H^3/E^2 can characterize elastic strain to failure, and resistance to plastic deformation, or, to some extent, fracture toughness [7], [34]. The H/E value was distinctly the highest at 2000 W for only laser-modified samples for both scanning speed values and for each surface modification. The H^3/E^2 increased at higher power values, 900 and 2000 W, for CNTs plus laser-modified samples (Figs. 8 and 9). Such results mean that the two-stage modification results in precipitation of some carbides, likely Ti_2C , whose density and dimensions become important with an increasing power followed by the occurrence of faster melting, faster diffusion of elements, and faster precipitation and even growth of precipitates. The more detailed microstructural investigations are in the course.

The performed research shows that the laser processing of the CNTs layers on the Ti13Nb13Zr alloy has a remarkable effect at a moderate laser power. Considering similar research, it is worth paying attention to the laser-made treatment performed in the $Ca(NO_3)_2$ solution in which the presence of two crystalline layers, melted and diffusion zones, has been noted [17]. For nitride and laser-melted surfaces, the remelted inner zone was 10 μm thick, and the martensitic outer zone appearing by the oxygen solid solution of oxygen was observed [19]. In similar conditions, the values of Young's modulus, elastic energy, and hardness significantly increased in the nitrated layer, followed by the heat-assisted zone [28] as well as some biological properties were enhanced when using a nanosecond laser for ablation treatment [38]. The observed relation can be then explained considering all results and possible processes occurring on the surface. Such processes occurring in the applied two-stage electrochemical-laser treatment include electrophoretic deposition of carbon nanotubes, melting and re-crystallization of the surface layer, formation of titanium carbides of a size determined by a local temperature decrease rate, and the associated change in local chemical composition, phase composition, and a level of residual stresses beneath the surface. Among all these processes, the precipitation of titanium carbides can be key phenomenon strongly related to energy flux. At low energy, the temperature is sufficiently high to form stable very small carbide phases, and at high energy following a local temperature increase, the carbides can grow

and coarse. Thus, at intermediate laser power and energy flux, the number and size of carbides are optimal to reach the highest hardness and resistance to plastic deformation, as determined from the nanoindentation tests. The precise description and modeling of these physical-chemical processes following by verification of the above hypothesis based on detailed microstructural investigations will be performed in the future.

5. Conclusions

The laser treatment of the Ti13Nb13Zr alloy causes a significant increase in roughness, hardness and resistance to elastic and plastic deformation described in terms of H/E and H^3/E^2 ratios. The effects are similar to those previously described for the other process parameters and can be attributed to the re-melting of the surface layer, rapid re-crystallization, and phase transformations.

The laser treatment of the surface previously deposited with multi-wall carbon nanotubes brings out divergent changes in the roughness and mechanical properties of the surface layer. They are substantially dependent on laser power and laser scanning speed. The most spectacular is strengthening observed at 900 W of laser energy and 6 mm/s of feed rate.

The prominent mechanical behavior at the intermediate laser power can be discussed in terms of temperature and energy density-dependent phenomena, in particular of the possible appearance of carbides in the surface layer in the region of lower energy fluence, and of the change in their growth and shape beneath the surface in the alloy laser-treated with excessive energy.

The proposed two-stage process is likely to substitute the carbonization of Ti and its alloys, as less time and cost-consuming, and can become important for all other metallic materials that have an appropriate melting temperature and can form carbide phases.

Acknowledgements

We wish to express our gratitude to Professor Andrzej Zieliński for his evaluation of the scientific quality of the research and manuscript, important comments, writing assistance, and proofreading, and to Dr. Michał Bartmański, and Dr. Grzegorz Gajowiec, for their technical aid in some experiments. We appreciate also the help of Marek Czarniecki during some tests.

Author contributions

Conceptualization, B.M.-M.; method, B.M.-M.; software, B.M.-M.; formal analysis, B.M.-M.; investigation, B.M.-M., J.S.; K.S.; writing – original draft, B.M.-M.; visualization, B.M.-M., J.S.; K.S.; supervision, B.M.-M. All authors have read and agreed to the published version of the manuscript.

References

- [1] ABDAL-HAY A., STAPLES R., ALHAZAA A., FOURNIER B., AL-GAWATI M., LEE R.S., IVANOVSKI S., *Fabrication of micropores on titanium implants using femtosecond laser technology: Perpendicular attachment of connective tissues as a pilot study*, *Opt. Laser Technol.*, 2022, 148, 107624, <https://doi.org/10.1016/j.optlastec.2021.107624>
- [2] ALKALLAS F.H., AHMED H.A., ADEL PASHAMEAH R., ALREFAE S.H., TOGHAN A., BEN GOUIDER TRABELSI A., MOSTAFA A.M., *Nonlinearity enhancement of Multi-walled carbon nanotube decorated with ZnO nanoparticles prepared by laser assisted method*, *Opt. Laser Technol.*, 2022, 155, 108444, <https://doi.org/10.1016/j.optlastec.2022.108444>
- [3] BAHIRAEI M., MAZAHERI Y., SHEIKHI M., HEIDARPOUR A., *Mechanism of TiC formation in laser surface treatment of the commercial pure titanium pre-coated by carbon using PVD process*, *J. Alloys Compd.*, 2020, 834, 155080, <https://doi.org/10.1016/j.jallcom.2020.155080>
- [4] AL BAROOT A., ELSAYED K.A., HALADU S.A., MAGAMI S.M., ALHESHIBRI M., ERCAN F., ÇEVİK E., AKHTAR S., A.MANDA A., KAYED T.S., ALTAMIMI N.A., ALSANEA A.A., AL-OTAIBI A.L., *One-pot synthesis of SnO₂ nanoparticles decorated multi-walled carbon nanotubes using pulsed laser ablation for photocatalytic applications*, *Opt. Laser Technol.*, 2023, 157, 108734, <https://doi.org/10.1016/j.optlastec.2022.108734>
- [5] CAI Q., LI G., WU B., XU S., WANG L., GUO Y., *Effect of TiC content on microstructure and properties of TiC / Ni60 coatings on Ti6Al4V alloy deposited by laser cladding*, *Opt. Laser Technol.*, 2024, 168, 109854, <https://doi.org/10.1016/j.optlastec.2023.109854>
- [6] CHAUHAN A.S., JHA J.S., TELRANDHE S., V S., GOKHALE A.A., MISHRA S.K., *Laser surface treatment of α - β titanium alloy to develop a β -rich phase with very high hardness*, *J. Mater. Process. Technol.*, 2021, 288, 116873, <https://doi.org/10.1016/j.jmatprotec.2020.116873>
- [7] CHEN X., DU Y., CHUNG Y.-W., *Commentary on using H/E and H^3/E^2 as proxies for fracture toughness of hard coatings*, *Thin Solid Films*, 2019, 688, 137265, <https://doi.org/10.1016/j.tsf.2019.04.040>
- [8] CHENG J., WANG S., TANG S., ZHOU J., CAO Z., WU D., LIU C., LI Y., *Controllable construction of laser-induced colorful patterns based on thermal energy transfer between carbon nanotubes substrate and polymer interface*, *Appl. Surf. Sci.*, 2023, 610, 155591, <https://doi.org/10.1016/j.apsusc.2022.155591>
- [9] DAI F., ZHANG Z., REN X., LU J., HUANG S., *Effects of laser shock peening with contacting foil on micro laser texturing surface of Ti6Al4V*, *Opt. Lasers Eng.*, 2018, 101, 99–105, <https://doi.org/10.1016/j.optlaseng.2017.09.024>
- [10] DOU H. QIANG, LIU H., XU S., CHEN Y., MIAO X., LÜ H., JIANG X., *Influence of laser fluences and scan speeds on the morphologies and wetting properties of titanium alloy*,

- Optik (Stuttg.), 2020, 224, 165443, <https://doi.org/10.1016/j.ijleo.2020.165443>
- [11] GERASIMENKO A.Y., KURILOVA U.E., SAVELYEV M.S., MURASHKO D.T., GLUKHOVA O.E., *Laser fabrication of composite layers from biopolymers with branched 3D networks of single-walled carbon nanotubes for cardiovascular implants*, Compos. Struct., 2021, 260, 113517, <https://doi.org/10.1016/j.compstruct.2020.113517>
- [12] GOPI D., SHINYOJOY E., SEKAR M., SURENDIRAN M., KAVITHA L., SAMPATH KUMAR T.S., *Development of carbon nanotubes reinforced hydroxyapatite composite coatings on titanium by electrodeposition method*, Corros. Sci., 2013, 73, 321–330, <https://doi.org/10.1016/j.corsci.2013.04.021>
- [13] GORODETSKIY D.V., KURENYA A.G., GUSEL'NIKOV A.V., BASKAKOVA K.I., SMIRNOV D.A., ARKHIPOV V.E., BULUSHEVA L.G., OKOTRUB A.V., *Laser beam patterning of carbon nanotube arrays for the work of electron field emitters in technical vacuum*, Mater. Sci. Eng. B Solid-State Mater. Adv. Technol., 2020, 262, 114691, <https://doi.org/10.1016/j.mseb.2020.114691>
- [14] GUO C., ZHANG M., HU J., *Fabrication of hierarchical structures on titanium alloy surfaces by nanosecond laser for wettability modification*, Opt. Laser Technol., 2022, 148, 107728. <https://doi.org/10.1016/j.optlastec.2021.107728>
- [15] GUO Y., XU L., LUAN J., WAN Y., LI R., *Effect of carbon nanotubes additive on tribocorrosion performance of micro-arc oxidized coatings on Ti6Al4V alloy*, Surfaces and Interfaces. 2022, 28, 101626, <https://doi.org/10.1016/j.surf.2021.101626>
- [16] HAN X., MA J., TIAN A., WANG Y., LI Y., DONG B., TONG X., MA X., *Surface modification techniques of titanium and titanium alloys for biomedical orthopaedics applications: A review*, Colloids Surfaces B Biointerfaces, 2023, 227, 113339, <https://doi.org/10.1016/j.colsurfb.2023.113339>
- [17] KATAHIRA K., EZURA A., OHKAWA K., KOMOTORI J., OHMORI H., *Generation of bio-compatible titanium alloy surfaces by laser-induced wet treatment*, CIRP Ann. – Manuf. Technol., 2016, 65, 237–240, <https://doi.org/10.1016/j.cirp.2016.04.053>
- [18] KUCZYŃSKA-ZEMŁA D., PURA J., PRZYBYSZEWSKI B., PISAREK M., GARBACZ H., *A comparative study of apatite growth and adhesion on a laser-functionalized titanium surface*, Tribol. Int., 2023, 182, 108338, <https://doi.org/10.1016/j.triboint.2023.108338>
- [19] KÜMMEL D., LINSLER D., SCHNEIDER R., SCHNEIDER J., *Surface engineering of a titanium alloy for tribological applications by nanosecond-pulsed laser*, Tribol. Int., 2020, 150, 106376, <https://doi.org/10.1016/j.triboint.2020.106376>
- [20] MAJKOWSKA-MARZEC B., ROGALA-WIELGUS D., BARTMAŃSKI M., BARTOSEWICZ B., ZIELIŃSKI A., *Comparison of Properties of the Hybrid and Bilayer MWCNTs – Hydroxyapatite Coatings on Ti Alloy*, Coatings, 2019, 9, 1–13.
- [21] MAJKOWSKA-MARZEC B., SYPNIEWSKA J., *Microstructure and Mechanical Properties of Laser Surface-Treated Ti13Nb13Zr Alloy with MWCNTs Coatings*, Adv. Mater. Sci., 2021, 21, 5–18, <https://doi.org/10.2478/adms-2021-0021>
- [22] MAJKOWSKA-MARZEC B., TECZAR P., BARTMAŃSKI M., BARTOSEWICZ B., JANKIEWICZ B.J., *Mechanical and corrosion properties of laser surface-treated Ti13Nb13Zr alloy with MWCNTs coatings*, Materials (Basel), 2020, 13, <https://doi.org/10.3390/ma13183991>
- [23] MAKURAT-KASPROLEWICZ B., OSSOWSKA A., *Recent advances in electrochemically surface treated titanium and its alloys for biomedical applications: A review of anodic and plasma electrolytic oxidation methods*, Mater. Today Commun., 2023, 34, 105425, <https://doi.org/10.1016/j.mtcomm.2023.105425>
- [24] MARCHEWKA J., JELEŃ P., DLUGOŃ E., SITARZ M., BŁAŻEWICZ M., *Spectroscopic investigation of the carbon nanotubes and polysiloxane coatings on titanium surface*, J. Mol. Struct., 2020, 1212, <https://doi.org/10.1016/j.molstruc.2020.128176>
- [25] PETRONIĆ S., ČOLIĆ K., ĐORĐEVIĆ B., MILOVANOVIĆ D., BURZIĆ M., VUČETIĆ F., *Effect of laser shock peening with and without protective coating on the microstructure and mechanical properties of Ti-alloy*, Opt. Lasers Eng., 2020, 129, <https://doi.org/10.1016/j.optlaseng.2020.106052>
- [26] ROGALA-WIELGUS D., MAJKOWSKA-MARZEC B., ZIELIŃSKI A., BARTMAŃSKI M., JANKIEWICZ B.J., *Mechanical behavior of bi-layer and dispersion coatings composed of several nanostructures on Ti13Nb13Zr alloy*, Materials (Basel), 2021, 14, 2905, <https://doi.org/10.3390/ma14112905>
- [27] RONOH K., MWEMA F., DABEES S., SOBOLA D., *Advances in sustainable grinding of different types of the titanium biomaterials for medical applications: A review*, Biomed. Eng. Adv., 2022, 4, 100047, <https://doi.org/10.1016/j.bea.2022.100047>
- [28] SHIRAZI H.A., CHAN C.W., LEE S., *Elastic-plastic properties of titanium and its alloys modified by fibre laser surface nitriding for orthopaedic implant applications*, J. Mech. Behav. Biomed. Mater., 2021, 124, 104802, <https://doi.org/10.1016/j.jmbbm.2021.104802>
- [29] SŁOMA M., WIERZBICKI M., SKALSKI A., *Composite powders with carbon nanotubes for laser printing of electronics*, Microelectron. Reliab., 2022, 136, <https://doi.org/10.1016/j.microrel.2022.114718>
- [30] SUN P., HU X., WEI G., WANG R., WANG Q., WANG H., WANG X., *Ti3O5 nanofilm on carbon nanotubes by pulse laser deposition: Enhanced electrochemical performance*, Appl. Surf. Sci., 2021, 548, <https://doi.org/10.1016/j.apsusc.2021.149269>
- [31] WANG Q., FANG B., LIU C., TU S.S., CHA L., RAMACHANDRAN C.S., *Characterization of plasma electrolytic oxidation coatings containing carbon nanotubes formed on selective laser melted AlSi10Mg alloy*, Surf. Coatings Technol., 2023, 454, 129145, <https://doi.org/10.1016/j.surfcoat.2022.129145>
- [32] WEISHEIT A., RITTINGHAUS S.K., DUTTA A., MAJUMDAR J.D., *Studies on the effect of composition and pre-heating on microstructure and mechanical properties of direct laser clad titanium aluminide*, Opt. Lasers Eng., 2020, 131, 106041, <https://doi.org/10.1016/j.optlaseng.2020.106041>
- [33] XU B., JIANG P., WANG Y., ZHAO J., GENG S., *Formation mechanism of aluminum and its carbides under wobbling laser melting injection with carbon nanotubes-SiC hybrid particles*, J. Mater. Process. Technol., 2023, 319, 118059, <https://doi.org/10.1016/j.jmatprotec.2023.118059>
- [34] YAN C., BOR B., PLUNKETT A., DOMÈNECH B., SCHNEIDER G.A., GIUNTINI D., *Nanoindentation of Supercrystalline Nanocomposites: Linear Relationship Between Elastic Modulus and Hardness*, Jom., 2022, 74, 2261–2276, <https://doi.org/10.1007/s11837-022-05283-3>
- [35] YANAN L., RONGLU S., WEI N., TIANGANG Z., YIWEN L., *Effects of CeO₂ on microstructure and properties of TiC/Ti 2 Ni reinforced Ti-based laser cladding composite coatings*, Opt. Lasers Eng., 2019, 120, 84–94, <https://doi.org/10.1016/j.optlaseng.2019.03.001>
- [36] YIN H., YANG J., ZHANG Y., CRILLY L., JACKSON R.L., LOU X., *Carbon nanotube (CNT) reinforced 316L stainless steel composites made by laser powder bed fusion: Microstructure and*

- wear response, *Wear*, 2022, 496–497, 204281, <https://doi.org/10.1016/j.wear.2022.204281>
- [37] YU A. HUA, XU W., LU X., TAMADDON M., LIU B. WEN, TIAN S. WEI, ZHANG C., MUGHAL M.A., ZHANG J. ZHEN, LIU C. ZONG, *Development and characterizations of graded porous titanium scaffolds via selective laser melting for orthopedics applications*, *Trans. Nonferrous Met. Soc. China (English Ed.)*, 2023, 33, 1755–1767, [https://doi.org/10.1016/S1003-6326\(23\)66219-3](https://doi.org/10.1016/S1003-6326(23)66219-3).
- [38] YU Z., ZHANG J., HU J., *Study on surface properties of nano-second laser textured plasma nitrided titanium alloy*, *Mater. Today Commun.*, 2022, 31, 103746, <https://doi.org/10.1016/j.mtcomm.2022.103746>.
- [39] ZHOU J.Z., HUANG S., ZUO L.D., MENG X.K., SHENG J., TIAN Q., HAN Y.H., ZHU W.L., *Effects of laser peening on residual stresses and fatigue crack growth properties of Ti-6Al-4V titanium alloy*, *Opt. Lasers Eng.*, 2014, 52, 189–194, <https://doi.org/10.1016/j.optlaseng.2013.06.011>.